Fast and Exact Simulation of Large Gaussian Lattice Systems in $\mathbb{R}^2$: Exploring the Limits

Tilmann Gneiting, Hana Ševčíková, Donald B. Percival, Martin Schlather and Yindeng Jiang[1]

Technical Report no. 477

Department of Statistics
University of Washington

April 4, 2005

Abstract

The circulant embedding technique allows for the fast and exact simulation of stationary and intrinsically stationary Gaussian random fields. The method uses periodic embeddings and relies on the fast Fourier transform. However, exact simulations require that the periodic embedding is nonnegative definite, which is frequently not the case for two-dimensional simulations. This work considers a suggestion by Michael Stein, who proposed nonnegative definite periodic embeddings based on suitably modified, compactly supported covariance functions. Theoretical support is given to this proposal, and software for its implementation is provided. The method yields exact simulations of planar Gaussian lattice systems with up to 10^6 lattice points for wide classes of processes, including those with powered exponential, Matérn and Cauchy covariances.

Key words: Circulant embedding; Compactly supported correlation function; Cut-off embedding; Fast Fourier transform; Gaussian random function; Intrinsic embedding; Torus process

1 Introduction

Simulated sample paths of Gaussian random fields are widely used in a variety of applications, ranging from computer graphics to environmental risk assessment and simulation studies. The discussion papers of Gotway (1994) and Gel, Raftery and Gneiting (2004), for instance, drew on simulated realizations of stationary Gaussian random fields to obtain predictive distributions of hydrological and meteorological quantities of interest. Davies and Hall (1999), Chan and Wood (2000) and Zhu and Stein (2002), among others, applied simulation studies to assess estimators

[1]Tilmann Gneiting is Associate Professor, Hana Ševčíková is Research Associate and Yindeng Jiang is Graduate Research Assistant, all at the Department of Statistics, University of Washington, Box 354322, Seattle, WA 98195-4322, USA. In Academic Year 2004/05, Tilmann Gneiting is on sabbatical leave at the Soil Physics Group, Universität Bayreuth, Universitätsstr. 30, 95440 Bayreuth, Germany. Donald B. Percival is Principal Mathematician at the Applied Physics Laboratory, University of Washington, Box 355640, Seattle, WA 98195-5640, USA. Martin Schlather is Associate Professor at Helmut-Schmidt-Universität, Institut für Statistik und Quantitative Ökonomik, Postfach 700822, 22008 Hamburg, Germany. This research was supported by the National Science Foundation under Awards 0134264 and 0222115. Author e-mail addresses: `tilmann@stat.washington.edu` (Gneiting), `hana@stat.washington.edu` (Ševčíková), `dbp@apl.washington.edu` (Percival), `schlath@hsu-hh.de` (Schlather), `yindeng@stat.washington.edu` (Jiang)

Table 1: Some Parametric Classes of Isotropic Covariance Functions. The Matérn class is defined in terms of the modified Bessel function, K_ν. We assume without loss of generality that $\varphi(0) = 1$.

Class	Functional Form	Parameters
Powered Exponential	$\varphi(t) = \exp(-(\theta t)^\alpha)$	$0 < \alpha \leq 2;\ \theta > 0$
Matérn	$\varphi(t) = \frac{2^{1-\nu}}{\Gamma(\nu)}\,(\theta t)^\nu K_\nu(\theta t)$	$\nu > 0;\ \theta > 0$
Cauchy	$\varphi(t) = (1 + (\theta t)^\alpha)^{-\beta/\alpha}$	$0 < \alpha \leq 2;\ \beta > 0;\ \theta > 0$

of fractal dimension for two-dimensional surface data. Simulation studies call for sampling techniques that are fast and exact in the sense that a method is computationally feasible and that the realizations have exactly the desired multivariate Gaussian distribution (Caccia et al. 1997). A comparison of the results in Section 6.1 of Chan and Wood (2000) and Section 4.4 of Zhu and Stein (2002) illustrates the conflicting inferences that the use of approximate and exact simulation may incur. Our work addresses this type of situation and explores the current computational limits of exact simulation.

A random field Z on $\mathbb{R}^d$ is said to be stationary if its mean is constant and $\text{cov}\{Z(\mathbf{x}), Z(\mathbf{y})\} = K(\mathbf{x}-\mathbf{y})$ for some function K on $\mathbb{R}^d$ and $\mathbf{x}, \mathbf{y} \in \mathbb{R}^d$. It is stationary and isotropic if $\text{cov}\{Z(\mathbf{x}), Z(\mathbf{y})\} = \varphi(|\mathbf{x}-\mathbf{y}|)$ for some function φ on $[0, \infty)$. Parametric models for isotropic covariance functions φ include the powered exponential class (Diggle, Tawn and Moyeed 1998), the Matérn class (Whittle 1954; Matérn 1986) and the Cauchy class (Gneiting and Schlather 2004). These parametric models are listed in Table 1. A slightly weaker assumption than stationarity is intrinsic stationarity. Specifically, a random field Z on $\mathbb{R}^d$ is said to be intrinsically stationary with variogram

$$\gamma(\mathbf{h}) = \frac{1}{2}\, E\Big(Z(\mathbf{x}) - Z(\mathbf{x}+\mathbf{h})\Big)^2, \qquad \mathbf{h} \in \mathbb{R}^d$$

if the increment process $I_\mathbf{h} = \{Z(\mathbf{x}) - Z(\mathbf{x}+\mathbf{h}) : \mathbf{x} \in \mathbb{R}^d\}$ is stationary for all lag vectors $\mathbf{h} \in \mathbb{R}^d$. A stationary random field Z with $\text{cov}\{Z(\mathbf{x}), Z(\mathbf{y})\} = K(\mathbf{x}-\mathbf{y})$ is intrinsically stationary with variogram $\gamma(\mathbf{h}) = K(\mathbf{0}) - K(\mathbf{h})$. However, not all intrinsically stationary random processes are stationary, with a fractional Brownian surface being one such example.

We consider the simulation of a stationary and isotropic Gaussian random field Z with $\text{cov}\{Z(\mathbf{x}), Z(\mathbf{y})\} = \varphi(|\mathbf{x}-\mathbf{y}|)$ on a square lattice of size $n \times n$ in $\mathbb{R}^2$. Analogues in higher dimensions and generalizations to rectangular lattices and other situations exist, but are of lesser relevance in applications. We order the lattice points row by row into a vector of size n^2, which then has a covariance matrix $\mathbf{C}$ that is block Toeplitz with each block being Toeplitz itself. The simulation problem consists of generating a Gaussian random vector in $\mathbb{R}^{n^2}$ with covariance matrix $\mathbf{C}$. One possibility is to do a Cholesky decomposition of the covariance matrix. This approach is exact, but fast algorithms for the Cholesky factorization of a block Toeplitz matrix still require $6n^5$ floating point operations or flops (Dietrich 1993). Dietrich and Newsam (1993, 1997) and Wood and Chan (1994) proposed the circulant embedding approach which embeds the simulation domain into a torus lattice, with significant computational advantages (Besag and Moran 1975; Rue and Held 2005, Section 2.6). Specifically, the covariance matrix of the periodic random field on the torus lattice is block circulant, with each block being circulant itself, which allows for the use of the fast Fourier transform. The result is a simulation algorithm with computational complexity of order $n^2 \log_2 n$.

Table 2: Computational Requirements for the Cholesky Decomposition and Circulant Embedding Methods of Simulating a Stationary Gaussian Random Field on a Square Lattice of Size $n \times n$. We adopt the 'new flop' terminology of Golub and van Loan (1996, p. 18) and suppose that an application of the fast Fourier transform to a vector of length m involves $5\,m \log_2 m$ flops (Golub and van Loan 1996, p. 190).

	Matrix Factorization (flops)	Each Realization (flops)	Storage (real values)
Standard Cholesky Decomposition	$\frac{1}{3}n^6$	n^4	$\frac{1}{2}n^4$
Efficient Cholesky Decomposition	$6n^5$	n^4	$2n^3$
Circulant Embedding	$40\,n^2 \log_2 2n$	$40\,n^2 \log_2 2n$	$8n^2$

A more detailed comparison of the computational requirements for the Cholesky decomposition and circulant embedding techniques is given in Table 2. A similar table in Kozintsev (1999) considers the standard implementation of the Cholesky decomposition only. Rue (2001) described a fast algorithm for the simulation of Gaussian Markov random fields that uses numerical techniques for sparse matrices. For square lattices with a $(2m+1) \times (2m+1)$ Markov neighborhood this algorithm has fixed costs of $n^4 m^2$ flops, and each realization requires another $2n^3 m$ flops.

The circulant embedding technique does not depend on a Markov structure and is both fast and exact, but requires the circulant embedding of the original covariance matrix to be nonnegative definite. For simulations in one dimension, various criteria are known that guarantee this under weak conditions (Dietrich and Newsam 1997; Gneiting 1998; Chilès and Delfiner 1999, p. 499; Craigmile 2003). However, for two-dimensional simulations the circulant embedding is frequently not nonnegative definite. Our work addresses this challenge and studies two proposals of Stein (2002a) that provide nonnegative definite embeddings and thereby guarantee exactness while maintaining computational efficiency.

The remainder of the paper is organized as follows. Section 2 reviews the standard circulant embedding approach and introduces Stein's proposals which depend on the construction of certain classes of compactly supported covariance functions. We give an example that compares the standard approach to Stein's suggestions, which we refer to as cut-off embedding and intrinsic embedding. Section 3 collects theoretical and numerical results on the aforementioned classes of compactly supported covariance functions. In Section 4 we describe the implementation of the cut-off and intrinsic embedding approaches within Version 1.2.5 of the R package RandomFields, and we explore the computational limits of exact simulation.

2 Circulant embedding

Suppose that we wish to simulate a stationary and isotropic Gaussian random field Z with covariance function $\mathrm{cov}\,\{Z(\mathbf{x}), Z(\mathbf{y})\} = \varphi(|\mathbf{x} - \mathbf{y}|)$ on a square lattice in $[0, s]^2$ with spacing s/n along each coordinate, where n is a positive integer. For convenience below we assume without loss of generality that $s = 1/\sqrt{2}$; hence, the lattice has a diagonal of length 1. The ideas and arguments can be generalized in many ways, but we restrict ourselves to a discussion of isotropic covariance functions and square lattices. The notation used below follows Stein (2002a).

Let Φ_2 denote the class of the continuous and isotropic covariance functions for random fields on $\mathbb{R}^2$. Specifically, a continuous function φ on $[0,\infty)$ belongs to Φ_2 if there exists a Gaussian random field Z with $\text{cov}\{Z(\mathbf{x}), Z(\mathbf{y})\} = \varphi(|\mathbf{x}-\mathbf{y}|)$ for $\mathbf{x}, \mathbf{y} \in \mathbb{R}^2$. For a function φ on $[0,\infty)$ and $r > 0$ define $P_r\varphi$ to be the function on $\mathbb{R}^2$ that has period $2r$ in each coordinate and is such that $P_r\varphi(\mathbf{x}) = \varphi(|\mathbf{x}|)$ for $\mathbf{x} \in [-r, r]^2$. For a positive integer m and $h > 0$, we define $\mathbf{C}(P_r\varphi; m, h)$ to be the $m^2 \times m^2$ covariance matrix for the vector of length m^2 formed by taking an $m \times m$ square lattice in $\mathbb{R}^2$, with spacing h along each coordinate, and ordering the lattice points row by row.

2.1 Standard, cut-off and intrinsic embedding

We now describe the standard implementation of the circulant embedding technique (Dietrich and Newsam 1993, 1997; Wood and Chan 1994). The periodicity of $P_s\varphi$ implies that $\mathbf{C}(P_s\varphi; 2n, s/n)$ has block circulant structure with each block being circulant itself. The eigenvalues of this matrix can be found by taking a discrete Fourier transform, and if n is highly composite this can be done very efficiently using the fast Fourier transform. If all eigenvalues are nonnegative, then an exact simulation of the periodic random field with covariance function $P_s\varphi$ on a $2n \times 2n$ lattice with spacing s/n along each coordinate can be obtained by generating a Gaussian random vector with $4n^2$ independent components and variances proportional to the eigenvalues, and applying the fast Fourier transform to this random vector. Essentially, this corresponds to simulating a Gaussian lattice process on the torus. Any set of points inside a square of side s can be extracted and provides the desired realization of a random field with covariance φ on a square lattice in $[0, s]^2$. The method involves an initial factorization of the block circulant matrix $\mathbf{C}(P_s\varphi; 2n, s/n)$ which can also be done by the fast Fourier transform, at a one-time cost of $40\,n^2 \log_2 2n$ flops. Each realization of the lattice process requires another $40\,n^2 \log_2 2n$ flops, and the storage requirement is $4n^2$ complex values, as summarized in Table 2. Dietrich and Newsam (1993, 1997), Wood and Chan (1994), Chan and Wood (1997) and Kozintsev (1999) gave detailed descriptions of the algorithm.

If $\mathbf{C}(P_s\varphi; 2n, s/n)$ has a negative eigenvalue, the standard embedding fails. Wood and Chan (1994, Section 4) suggested an approximative embedding procedure that does not require the matrix $\mathbf{C}(P_s\varphi; 2n, s/n)$ to be nonnegative definite. However, this variant of the circulant embedding method does not provide exact simulations. To retain exactness, Wood and Chan (1994) and Dietrich and Newsam (1993, 1997) proposed the following approach: Pick some $c > 1$ for which cn is an integer and compute the eigenvalues of the block circulant matrix $\mathbf{C}(P_{cs}\varphi; 2cn, s/n)$. Proposition 2 of Wood and Chan (1994) shows that under mild regularity conditions $\mathbf{C}(P_{cs}\varphi; 2cn, s/n)$ will be nonnegative definite if c is sufficiently large. The fast Fourier transform can be applied as above, and we obtain exact realizations on the original lattice, by extracting any set of points inside a square of side s. However, the computational requirements of the circulant embedding method grow quadratically in c, and in many cases c needs to be chosen excessively large. In this situation, exact simulation with the standard circulant embedding technique fails, and we resort to Stein's (2002a) proposals for cut-off embedding and intrinsic embedding.

We first describe the *cut-off embedding* approach to which Stein (2002a) alluded at the end of his Section 4. Rather than simulating the covariance function φ directly, cut-off embedding turns to functions of the form

$$\rho(t) = \begin{cases} \varphi(t), & 0 \le t \le 1, \\ \psi(t), & 1 \le t \le r, \\ 0, & t \ge r, \end{cases} \tag{1}$$

where $r \ge 1$ and ψ is any function, but chosen such that ρ belongs to the class Φ_2 of the continuous, stationary and isotropic covariance functions on $\mathbb{R}^2$. Let $d \geq r/s$ be such that dn is a highly composite integer. If $\rho \in \Phi_2$ then the facts that $d \geq r/s$ and $\rho(t) = 0$ for $t \geq r$ imply that $P_{ds}\rho$ is a covariance function in $\mathbb{R}^2$ (Dietrich and Newsam 1993). Hence, the block circulant matrix $\mathbf{C}(P_{ds}\rho; 2dn, s/n)$ is nonnegative definite, and the standard circulant embedding technique applies to this modified matrix. To obtain exact realizations on the original square lattice, we extract any set of points inside a square of side s. If d can be chosen smaller than the c required to make $\mathbf{C}(P_{cs}\varphi; 2cn, s/n)$ nonnegative definite, the cut-off embedding approach allows for exact simulations at reduced computational cost.

The other approach proposed by Stein (2002a), to which we refer as *intrinsic embedding*, uses functions of the form

$$\sigma_r(t) = \begin{cases} a_0 + a_2 t^2 + \varphi(t), & 0 \leq t \leq 1, \\ \psi(t), & 1 \leq t \leq r, \\ 0, & t \geq r, \end{cases} \tag{2}$$

where $r \geq 1$, $a_0 \in \mathbb{R}$, and $a_2 \geq 0$ are constants and ψ is any function, chosen such that σ_r belongs to the class Φ_2. Let $d \geq r/s$ be such that dn is a highly composite integer. If $\sigma_r \in \Phi_2$, the aforementioned argument shows that $P_{ds}\sigma_r$ is a covariance function in $\mathbb{R}^2$ and that $\mathbf{C}(P_{ds}\sigma_r; 2dn, s/n)$ is nonnegative definite. We apply the standard circulant embedding method based on the matrix $\mathbf{C}(P_{ds}\sigma_r; 2dn, s/n)$ and obtain an exact simulation of a stationary and isotropic Gaussian random field Z_σ with $\text{cov}\{Z_\sigma(\mathbf{x}), Z_\sigma(\mathbf{y})\} = \sigma_r(|\mathbf{x} - \mathbf{y}|)$. Let X_1 and X_2 be independent Gaussian random variables with mean 0 and variance $2a_2$ that are independent of Z_σ. We write $\mathbf{x} = (x_1, x_2) \in \mathbb{R}^2$ and restrict the random field $Z(\mathbf{x}) = Z_\sigma(\mathbf{x}) + x_1 X_1 + x_2 X_2$ to the square lattice $\mathbf{S}$ with spacing s/n in $[0, s]^2$. Then $Z(\mathbf{x})$, $\mathbf{x} \in \mathbf{S}$, is an intrinsically stationary process and has exactly the desired variogram structure, namely

$$\frac{1}{2} E\left(Z(\mathbf{x}) - Z(\mathbf{y})\right)^2 = \varphi(0) - \varphi(|\mathbf{x} - \mathbf{y}|), \qquad \mathbf{x}, \mathbf{y} \in \mathbf{S}.$$

In various types of applications, such as simulation studies for increment-based estimators of fractal dimension, the reproduction of the variogram structure suffices, and if d can be chosen smaller than the c required to make $\mathbf{C}(P_{cs}\varphi; 2cn, s/n)$ nonnegative definite, the intrinsic embedding technique allows for computationally efficient exact simulation. Stein (2002a) studied this approach in the special case of the exponential covariance, $\varphi(t) = \exp(-\theta t)$, but did not consider other covariance functions.

2.2 Example

We now give an explicit example of standard, cut-off and intrinsic embedding. Suppose that we wish to simulate a stationary and isotropic Gaussian random field Z with powered exponential covariance function, $\text{cov}\{Z(\mathbf{x}), Z(\mathbf{y})\} = \exp(-|\mathbf{x} - \mathbf{y}|^{1/2})$ on a square lattice on $[0, s]^2$ with spacing $s/256$ along each coordinate, where $s = 1/\sqrt{2}$. Exact simulation using the Cholesky decomposition takes at least $3 \cdot 2^{41}$ flops for the matrix factorization and 2^{32} flops for each realization.

Applying the standard circulant embedding technique requires that we find a number $c \in [1, 8]$ such that $256c$ is a highly composite integer and the eigenvalues of the block circulant matrix $\mathbf{C}(P_{cs}\varphi; 2c \cdot 256, s/256)$ are nonnegative, where $\varphi(t) = \exp(-t^{1/2})$. The requirement that $c \leq 8$ stems from the storage requirement of $8 \cdot (256c)^2 = 2^{19}c^2$ real values (see Table 2) and storage limitations (see Section 4 below). Table 3 shows the smallest eigenvalue of $\mathbf{C}(P_{cs}\varphi; 2c \cdot 256, s/256)$ for $c = 1, 2, 4$ and 8. None of the matrices is nonnegative definite and the standard circulant embedding approach fails.

Table 3: Smallest Eigenvalue, $\lambda_{\min}(c)$, and Number of Negative Eigenvalues, $n_-(c)$, of the Block Circulant Matrix $\mathbf{C}(P_{cs}\varphi, 2c \cdot 256, s/256)$ where $s = 1/\sqrt{2}$ and $\varphi(t) = \exp(-t^{1/2})$. The matrix is of size $n(c) \times n(c)$, and the relative frequency of negative eigenvalues, $n_-(c)/n(c)^2$, decays approximately like $1/n(c)$.

c	$\lambda_{\min}(c)$	$n_-(c)$	$n(c)$
1	−10.90	502	512
2	−9.64	1 002	1 024
4	−3.60	1 986	2 048
8	−0.43	3 786	4 096

Instead, we consider the cut-off embedding approach with the function

$$\rho(t) = \begin{cases} \exp\left(-t^{1/2}\right), & 0 \le t \le 1, \\ \frac{1}{e}\left(2 - t^{1/2}\right), & 1 \le t \le 4, \\ 0, & t \ge 4. \end{cases} \tag{3}$$

Theorem 1 below shows that ρ belongs to the class Φ_2, and it follows that $\mathbf{C}(P_{ds}\rho; 2d \cdot 256, s/256)$ is nonnegative definite if $d \ge 4\sqrt{2}$. The standard circulant embedding technique applied to the modified matrix $\mathbf{C}(P_{8s}\rho; 2 \cdot 8 \cdot 256, s/256)$ yields $(2 \cdot 8)^2 = 256$ distinct exact realizations on the original lattice extracted from 256 disjoint squares of side 1 each. The realizations are dependent and typically only one of them is used. The computational cost is $15 \cdot 2^{27}$ flops for the matrix factorization and for each simulation.

Alternatively, we might turn to the intrinsic embedding approach with the function

$$\sigma_1(t) = \begin{cases} \exp\left(-t^{1/2}\right) - \frac{5}{4e} + \frac{1}{4e}t^2, & 0 \le t \le 1, \\ 0, & t \ge 1. \end{cases} \tag{4}$$

Theorem 3 below implies that σ_1 belongs to the class Φ_2, and it follows that $\mathbf{C}(P_{ds}\sigma_1; 2d \cdot 256, s/256)$ is nonnegative definite if $d \ge \sqrt{2}$. The standard circulant embedding technique applies to the matrix $\mathbf{C}(P_{2s}\sigma_1, 2 \cdot 2 \cdot 256, s/256)$ and we obtain realizations of an intrinsically stationary Gaussian random field with exactly the desired variogram structure, as described above. The computational cost is reduced to $5^2 \cdot 2^{22}$ flops for the matrix factorization and for each simulation. However, in contrast to the cut-off embedding approach, the simulated process is nonstationary.

3 Compactly supported covariance functions

The cut-off embedding and intrinsic embedding approaches depend on the availability of compactly supported functions that are of the form (1) or (2), respectively, and belong to the class Φ_2. This section provides analytical and numerical devices for the construction of such functions. Supplementary information on compactly supported covariance functions can be found in Gneiting (2002) and the references therein.

3.1 Criteria of the Pólya type

A function φ on $[0,\infty)$ belongs to the class Φ_2 of the continuous, stationary and isotropic covariance functions in $\mathbb{R}^2$ if and only if it is of the form

$$\varphi(t) = \int_{[0,\infty)} J_0(rt)\,\mathrm{d}F(r) \tag{5}$$

for $t \geq 0$, where J_0 is a Bessel function and F is nondecreasing and bounded. If φ has compact support, then it is of the form (5) if and only if the Bessel integral

$$f(r) = \frac{1}{2\pi} \int_{[0,\infty)} t\,\varphi(t)\,J_0(tr)\,\mathrm{d}t \tag{6}$$

is nonnegative for all $r > 0$ (Stein 1999, Section 2.10). Unfortunately, it is quite difficult in general to prove the nonnegativity of the Bessel integral in (6). Stein (2002a, 2002b) took this ambitious route in a number of instances, and the length and complexity of his proofs attest to the difficulty of the approach.

Instead, we apply criteria of the Pólya type. Suppose that φ is a continuous function on $[0,\infty)$ with $\varphi(0) > 0$ and $\lim_{t\to\infty} \varphi(t) = 0$. The celebrated criterion of Pólya (Chilès and Delfiner 1999, p. 66; Stein 1999, p. 54) states that if φ is convex then there exists a stationary Gaussian process Z on $\mathbb{R}$ such that $\mathrm{cov}\{Z(x), Z(y)\} = \varphi(|x-y|)$. Table 4 lists analogues of Pólya's criterion that apply to stationary random fields in $\mathbb{R}^2$. These results were proved in Gneiting (1999a, 1999b, 2001) and, using the first criterion as an example, can be applied as follows: If $\varphi(t^2)$ is convex or, almost equivalently, if $\varphi''(t)$ exists and $\varphi'(t) + 2t\varphi''(t) \geq 0$ for $t > 0$ then there exists a stationary Gaussian process Z on $\mathbb{R}^2$ such that $\mathrm{cov}\{Z(\mathbf{x}), Z(\mathbf{y})\} = \varphi(|\mathbf{x}-\mathbf{y}|)$; that is, $\varphi \in \Phi_2$. The second column in Table 4 is to be understood as follows. Suppose there exist positive numbers α and λ such that

$$\lim_{t\to 0} t^{-\alpha}\,(\varphi(0) - \varphi(t)) = \lambda. \tag{7}$$

Then a necessary (but not sufficient) requirement for the convexity or nonnegativity condition to hold is that the above be true with α restricted as stated in the table. Powered exponential, Matérn and Cauchy covariances all satisfy the relationship (7), with α given by the parameterization of Table 1 or, in the case of the Matérn class, with $\alpha = 2\min(\nu, 1)$.

Criteria of the Pólya type occasionally allow for vastly simplified proofs, and they can be used to demonstrate results that cannot be proved otherwise. In the following we use criteria of Pólya type to show that functions of the form (1) or (2) belong to the class Φ_2. In cases in which the criteria do not apply we follow Stein (2002a) and report the results of numerical experiments.

3.2 Cut-off embedding

The cut-off embedding technique employs elements of the class Φ_2 that are of the form

$$\rho(t) = \begin{cases} \varphi(t), & 0 \leq t \leq 1, \\ \psi(t), & 1 \leq t \leq r, \\ 0, & t \geq r, \end{cases}$$

where φ is a standard covariance model, say from the powered exponential, Matérn or Cauchy class. Theorems 1 and 2 below concern the cases in which $\psi(t) = b\,(r^{1/2} - t^{1/2})$ and $\psi(t) = b\,(r-t)^2$,

Table 4: Criteria of the Pólya Type for Isotropic Covariance Functions in $\mathbb{R}^2$. A continuous function φ on $[0,\infty)$ belongs to the class Φ_2 if $\varphi(0)$ is positive, $\lim_{t\to\infty}\varphi(t)=0$, and if the convexity or the nonnegativity condition in the table holds.

Convexity Condition Nonnegativity Condition	Requires	Reference
$\varphi(t^2)$ convex $\varphi'(t)+2t\,\varphi''(t)\geq 0$	$\alpha\leq\frac{1}{2}$	Gneiting (1999a)
$-\varphi'(t^{1/2})$ convex $\varphi''(t)-t\,\varphi'''(t)\geq 0$	$\alpha\leq 1$	Gneiting (1999b)
$t^{-2}\left(2\,\varphi'(t^{1/2})-2t^{1/2}\varphi''(t^{1/2})+t\,\varphi'''(t^{1/2})\right)$ convex $48\,(\varphi''(t)-\varphi'(t))-24t^2\,\varphi'''(t)+7t\,\varphi^{(iv)}(t)-t^4\,\varphi^{(v)}(t)\geq 0$	$\alpha\leq 2$	Gneiting (2001)

respectively. We experimented with various other forms of ψ, but the results were generally of limited use. For instance, analogues of Theorem 1 and Theorem 2 apply when $\psi(t)=b\,(r^c-t^c)$ where $0<c\leq\frac{1}{2}$, and $\psi(t)=b\,(r-t)^c$ where $c\geq 2$, respectively, with b and r chosen such that ρ is smooth. However, the cut-off embedding approach calls for small values of the cut-off, r, and the latter is mimimal when $c=\frac{1}{2}$ and $c=2$, respectively.

Theorem 1 *Let φ be a continuous function on $[0,1]$ such that $\varphi(t^2)$ is positive and convex and $\varphi'(1)$ is negative. Then the function ρ on $[0,\infty)$ defined by*

$$\rho(t)=\begin{cases}\varphi(t), & 0\leq t\leq 1,\\ b\,(r^{1/2}-t^{1/2}), & 1\leq t\leq r,\\ 0, & t\geq r,\end{cases} \tag{8}$$

where

$$r=\left(1-\frac{1}{2}\,\frac{\varphi(1)}{\varphi'(1)}\right)^2, \qquad b=-2\,\varphi'(1), \tag{9}$$

belongs to the class Φ_2.

Note that r and b are chosen such that ρ is continuous and differentiable at $t=1$. We skip the proof of Theorem 1, which consists in a straightforward reduction to the first criterion in Table 4. For covariances of powered exponential type, $\varphi(t)=\exp(-(\theta t)^\alpha)$, and for covariances of Cauchy type, $\varphi(t)=(1+(\theta t)^\alpha)^{-\beta/\alpha}$, the conditions of the theorem are satisfied if and only if $\alpha\leq\frac{1}{2}$. If φ is powered exponential with $\alpha=\frac{1}{2}$ and $\theta=1$, we recover eq. (3). If φ belongs to the Matérn class, that is, if

$$\varphi(t)=\frac{2^{1-\nu}}{\Gamma(\nu)}\,(\theta t)^\nu K_\nu(\theta t),$$

where K_ν is a modified Bessel function of index $\nu>0$, we get

$$\varphi'(t)=-\frac{2^{1-\nu}}{\Gamma(\nu)}\,\theta^{\nu+1}\,t^\nu\,K_{\nu-1}(\theta t).$$

It is not difficult to show that the conditions of Theorem 1 are violated if $\nu > \frac{1}{4}$. We believe but have not been able to prove that they are satisfied if $\nu \leq \frac{1}{4}$. Clearly, the conditions are sufficient only, and a function defined by (8) and (9) might belong to the class Φ_2 even though the assumptions of the theorem are violated.

Theorem 2 *Let φ be a continuous function on $[0,1]$ such that $\varphi'(t^{1/2})$ exists and is concave, $\varphi(1)$ is positive, $\varphi'(1)$ is negative, and*

$$2\,\varphi(1)\,\varphi''(1) \geq \left(\varphi'(1)\right)^2.$$

Then the function ρ on $[0,\infty)$ defined by

$$\rho(t) = \begin{cases} \varphi(t), & 0 \leq t \leq 1, \\ b\,(r-t)^2, & 1 \leq t \leq r, \\ 0, & t \geq r, \end{cases} \tag{10}$$

where

$$r = 1 - 2\,\frac{\varphi(1)}{\varphi'(1)}, \qquad b = \left(\frac{1}{2}\,\frac{\varphi'(1)}{\varphi(1)}\right)^2 \varphi(1), \tag{11}$$

belongs to the class Φ_2.

This result is proved by a reduction to the second criterion of Pólya type in Table 4. If φ is a powered exponential or a Cauchy covariance, the conditions of Theorem 2 are satisfied if and only if $\alpha \leq 1$. If $\alpha \leq \frac{1}{2}$ both (8) and (10) yield valid covariances, and we prefer the function with the smaller value of the cut-off, r. For powered exponential covariances, for example, (10) has a smaller cut-off than (8) if $4\,\alpha\,\theta^{\alpha} > 1$. If φ is a Matérn covariance, we conjecture that the assumptions of the theorem hold if and only if $\nu \leq \frac{1}{2}$. Again, the conditions are sufficient only, and a function defined by (10) and (11) might well belong to the class Φ_2 even though the assumptions of Theorem 2 are violated.

When $\alpha > 1$ for covariances of powered exponential and Cauchy type or $\nu > \frac{1}{2}$ for Matérn covariances, the first two criteria in Table 4 do not apply, and our attempts to invoke the third criterion have been of limited success. Partial results are available, but they are highly technical and depend on systems of equations that require numerical solution. Instead, we report numerical results. Figures 1 and 2 illustrate the parameter ranges for which the block circulant matrix $\mathbf{C}(P_r\,\rho, 2 \cdot 2048, r/2048)$ is nonnegative definite, where ρ is defined by (10) and (11) and φ is of the powered exponential and Matérn type, respectively. The associated numerical value of the cut-off is illustrated, too. The results for Cauchy covariances with $\beta = 1$ or $\beta = 2$ are similar to those for the powered exponential class.

3.3 Intrinsic embedding

The intrinsic embedding approach calls for elements of the class Φ_2 that are of the form (2), where again φ is a standard covariance model. Following Stein (2002a), we consider

$$\sigma_r(t) = \begin{cases} a_0 + a_2 t^2 + \varphi(t), & 0 \leq t \leq 1, \\ b\,(r-t)^3/t, & 1 \leq t \leq r, \\ 0, & t \geq r, \end{cases} \tag{12}$$

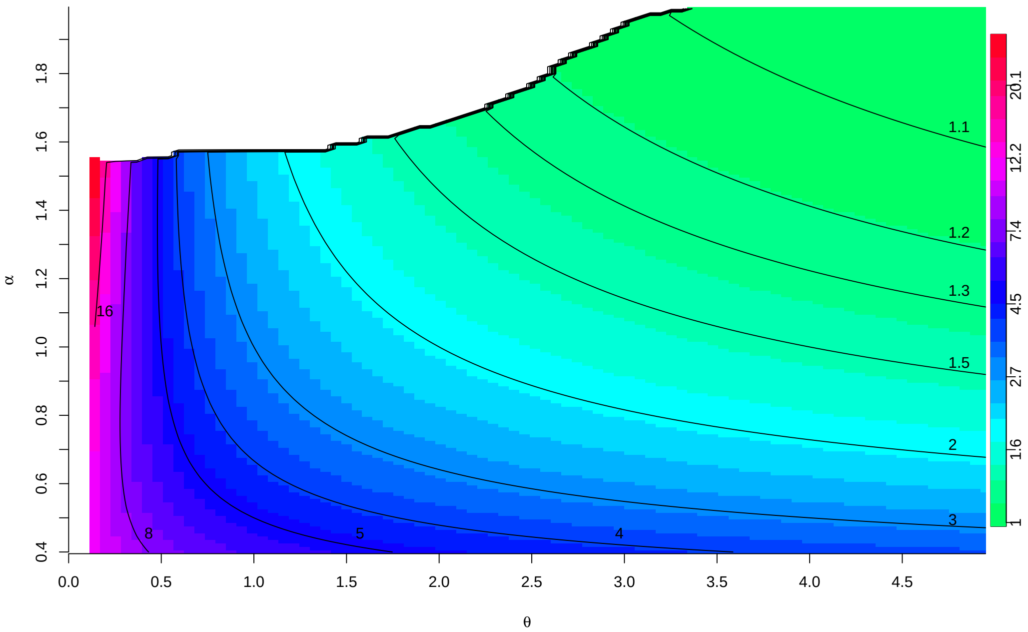

Figure 1: Cut-off Embedding for the Powered Exponential Class. We consider the block circulant matrix $\mathbf{C}(P_r\rho, 2\cdot 2048, r/2048)$ where ρ is given by (10) and (11) and φ is powered exponential with shape parameter α and scale parameter θ. The graph divides the (α, θ) plane into a lower area (coloured), for which this matrix is nonnegative definite, and an upper area (white), for which it is not. The color scheme corresponds to the associated numerical value of the cut-off, r, which is also indicated by the isolines.

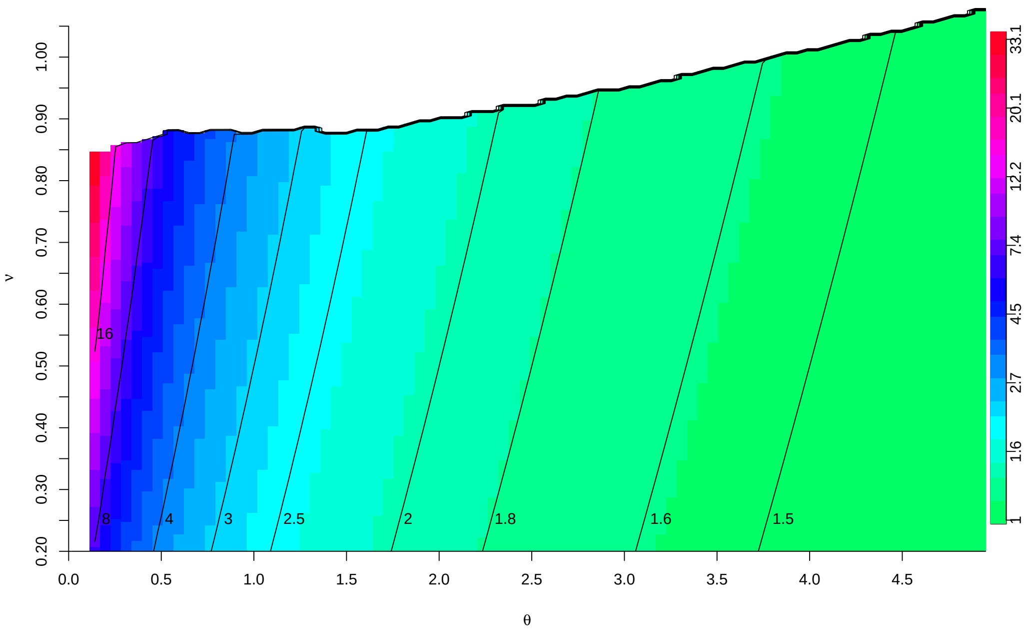

Figure 2: Same as Figure 1 for Matérn Covariances With Shape Parameter ν and Scale Parameter θ.

where the cutoff, $r \geq 1$, is fixed and $a_0 \in \mathbb{R}$, $a_2 \geq 0$ and $b \geq 0$ are chosen such that σ_r is smooth at $t = 1$; that is,

$$a_0 = \frac{1}{2}\frac{r-1}{r+1}\,\varphi''(1) + \frac{1}{r+1}\,\varphi'(1) - \varphi(1), \qquad a_2 = \frac{\varphi''(1) - \varphi'(1)}{3r(r+1)} - \frac{1}{3}\,\varphi'(1) - \frac{1}{6}\,\varphi''(1) \tag{13}$$

and

$$b = \frac{\varphi''(1) - \varphi'(1)}{3\,r\,(r^2-1)}. \tag{14}$$

Small values of the cut-off are preferable, and for the minimal value, $r = 1$, eqs. (12) and (13) reduce to (15) and (16) below, respectively. We have the following result.

Theorem 3 *Let φ be a continuous function on $[0,1]$ such that $-\varphi'(t^{1/2})$ exists and is convex, $\varphi(1)$ is positive, $\varphi'(1)$ is negative, $\varphi''(1)$ is positive, and*

$$\frac{1}{2}\,\varphi'(1) + \varphi(0) - \varphi(1) > 0.$$

Then the function σ_1 on $[0,\infty)$ defined by

$$\sigma_1(t) = \begin{cases} a_0 + a_2 t^2 + \varphi(t), & 0 \leq t \leq 1, \\ 0, & t \geq 1, \end{cases} \tag{15}$$

where

$$a_0 = \frac{1}{2}\,\varphi'(1) - \varphi(1), \qquad a_2 = -\frac{1}{2}\,\varphi'(1), \tag{16}$$

belongs to the class Φ_2.

A similar theorem with almost identical assumptions holds for σ_r and $r \geq 1$. This more general result is also proved by a reduction to the second criterion in Table 4, and we leave the details to the reader. If φ is a powered exponential or a Cauchy covariance, the conditions of Theorem 3 are satisfied if and only if $\alpha \leq 1$. In particular, the function

$$\sigma_1(t) = \begin{cases} \exp(-\theta t) - \left(1 + \frac{\theta}{2}\right) e^{-\theta} + \frac{\theta}{2} e^{-\theta}\, t^2, & 0 \leq t \leq 1, \\ 0, & t \geq 1, \end{cases}$$

belongs to the class Φ_2, which proves a conjecture of Stein (2002a, p. 593). If φ is powered exponential with $\alpha = \frac{1}{2}$ and $\theta = 1$, eqs. (15) and (16) recover (4). For Matérn covariances we conjecture that the conditions of Theorem 3 are satisfied if and only if $\nu \leq \frac{1}{2}$. Again, the conditions are sufficient but not necessary.

If $\alpha > 1$ or $\nu > \frac{1}{2}$, respectively, analytical results are not available, and we report on numerical experiments instead. Generally, our experiments suggest that, if $\mathbf{C}(P_r\sigma_r, 2n, r/n)$ is nonnegative definite, then $\mathbf{C}(P_{r'}\sigma_{r'}, 2n', r'/n')$ is nonnegative definite for $n' \leq n$ and $r' \geq r$. Furthermore, our experiments indicate that, if $\mathbf{C}(P_2\sigma_2, 2n, 2/n)$ fails to be nonnegative definite, then $\mathbf{C}(P_r\sigma_r, rn, 2/n)$ is not nonnegative definite for $r \geq 2$ either. Figure 3 summarizes the results for the block circulant matrix $\mathbf{C}(P_r\sigma_r, 2 \cdot 2048, r/2048)$ and the powered exponential class. For instance, if $\theta = 1$ and $\alpha \leq 1.7$, then this matrix is nonnegative definite if $r \geq 1.4$. If $\theta = 1$ and $\alpha = 1.9$, we cannot find an r that makes this matrix nonnegative definite. Figure 4 shows the respective results for the Matérn class. The results for Cauchy covariances with $\beta = 1$ or $\beta = 2$ are similar to those for the powered exponential class.

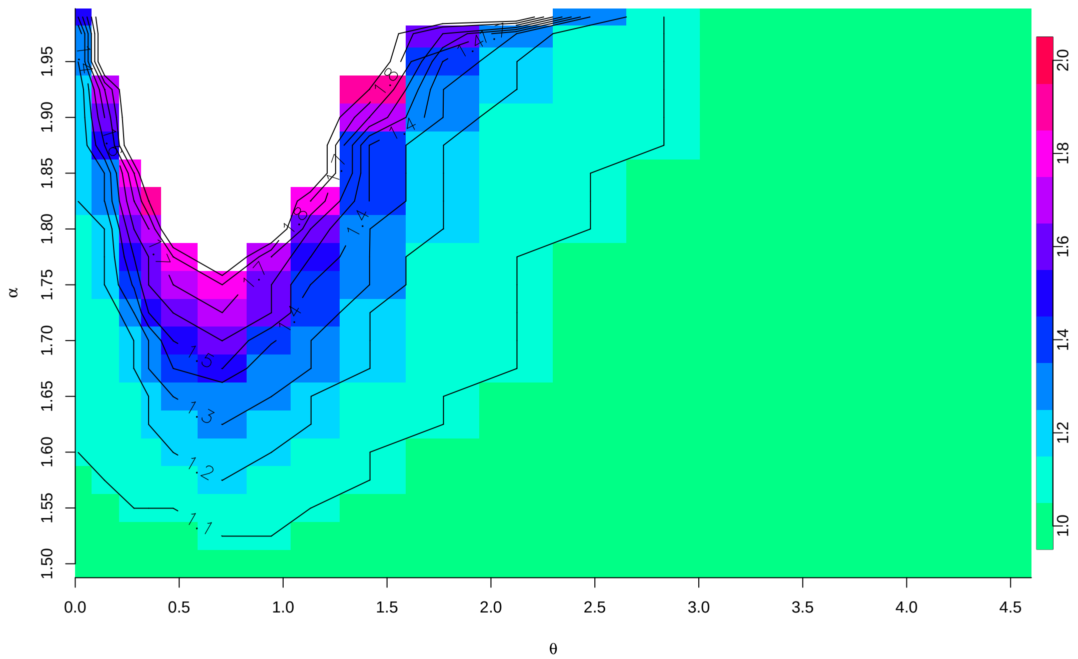

Figure 3: Intrinsic Embedding for the Powered Exponential Class. We consider the block circulant matrix $\mathbf{C}(P_r\sigma_r, 2\cdot 2048, r/2048)$ where σ_r is given by (12), (13) and (14), and φ is powered exponential with shape parameter α and scale parameter θ, respectively. The isolines show the smallest value of r that makes the matrix nonnegative definite. The white area in the (θ, α) plane marks the parameter combinations for which no such r could be found.

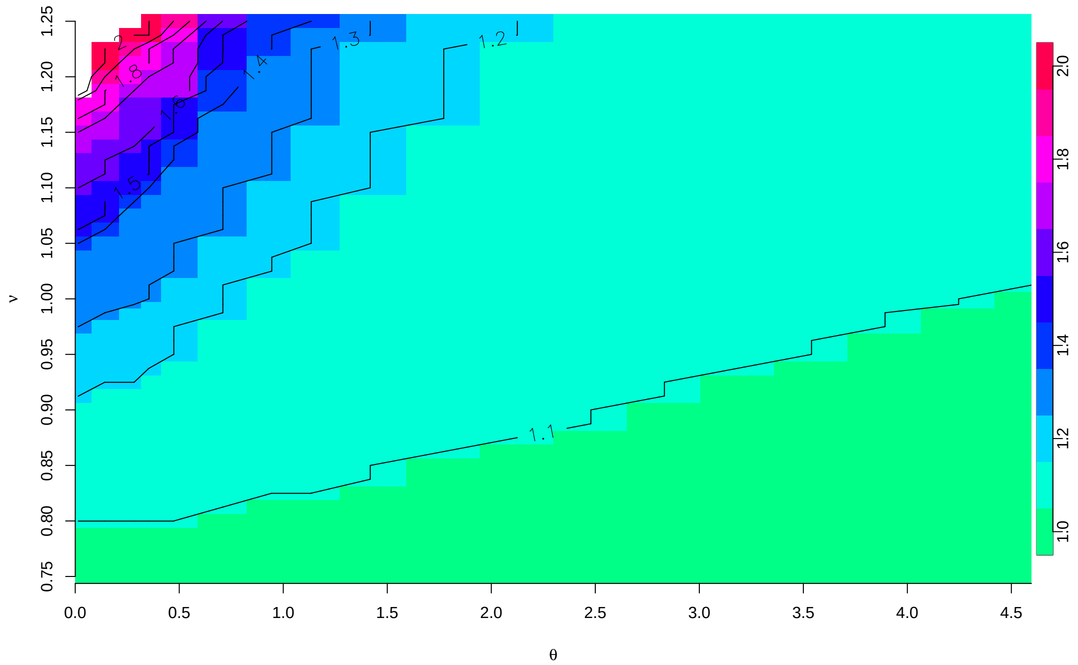

Figure 4: Same as Figure 3 for Matérn Covariances with Shape Parameter ν and Scale Parameter θ.

4 Implementation

We now describe strategies for choosing a simulation algorithm, and we discuss the current computational limits of exact simulation. The cut-off embedding and intrinsic embedding techniques have been implemented in Version 1.2.5 of the RandomFields package (Schlather 2001) for the R language (Ihaka and Gentleman 1996), and we give an example of using this package.

4.1 Choice of simulation algorithm

Recall that we wish to simulate a Gaussian surface Z with $\text{cov}\{Z(\mathbf{x}),\, Z(\mathbf{y})\} = \varphi(|\mathbf{x}-\mathbf{y}|)$ on a square lattice of size $n \times n$, with spacing s/n along each coordinate. Without loss of generality we can assume that $s = 1/\sqrt{2}$, which avoids a scaling argument in the use of the above results. Sophisticated users of the RandomFields package will specify the desired simulation technique directly, and in Section 4.3 below we give an example of how this can be done. For less experienced users, the `GaussRF` function provides an automated search for a suitable simulation algorithm. In describing this search, we suppose that the fast Fourier transform can be applied to square matrices of size at most $2m \times 2m$ where m is a power of 2. On our 512 MB RAM machine we found $m = 2\,048$ to be a reasonable choice; $m = 4\,096$ was still feasible but caused discontinuities in the response time of the system.

If n is small, say $n \leq 64$, the Cholesky decomposition technique applies and performs well. For larger systems, the standard embedding approach is the most straightforward and the most easily applicable among the three variants of the circulant embedding technique. Hence, the automated search for an exact simulation algorithm considers the standard approach first, by checking whether the block circulant matrix $\mathbf{C}(P_{cs}\varphi; 2cn, s/n)$ is nonnegative definite for some $c \in [1, m/n]$ such that cn is a highly composite integer. If the standard embedding approach fails, the search proceeds based on the user's preferences. If the `GaussRF` parameter `stationary.only` is set to `FALSE`, stationarity is not essential, and the intrinsic embedding technique provides a particularly efficient alternative. Let c be such that cn is the smallest power of two greater than or equal to n/s, and define σ_{cs} as in (12). The `GaussRF` function uses the intrinsic embedding technique if $cn \leq m$ and the block circulant matrix $\mathbf{C}(P_{cs}\sigma_{cs}; 2cn, s/n)$ is nonnegative definite, or if $2cn \leq m$ and $\mathbf{C}(P_{2cs}\sigma_{2cs}; 2 \cdot 2cn, s/n)$ is nonnegative definite. If the intrinsic embedding approach fails, or if the parameter `stationary.only` is set to `TRUE`, the search turns to the cut-off embedding approach. If (9) or (11) yield a cut-off, r, such that $r/s \leq m/n$, we define ρ by (8) or (10), respectively, find the smallest $c \geq r/s$ such that cn is a highly composite integer, and check whether the block circulant matrix $\mathbf{C}(P_{cs}\rho; 2cn, s/n)$ is nonnegative definite. There is no guarantee that any of the approaches work, and exact simulation may not be feasible.

At various stages in this search, block circulant matrices need to be checked for nonnegative definiteness. Whenever possible, we use theoretical results or look-up tables for doing this. A less computationally efficient alternative is to determine the eigenvalues numerically using the fast Fourier transform. In this numerical test, we consider a block circulant matrix to be nonnegative definite if the real parts of all eigenvalues are nonnegative and the moduli of the imaginary parts are small (10^{-8} or less, thereby allowing for numerical noise). Clearly, refinements in the automated search are possible. To simulate random fields with standard covariance structures, for instance, one might turn to the intrinsic embedding and cut-off embedding approaches directly, without attempting to invoke the standard approach. Applications in environmental risk assessment and simulation studies sometimes require large numbers of realizations. In these cases, parallel computing provides further improvements in computational feasibility and efficiency (Ševčíková 2004).

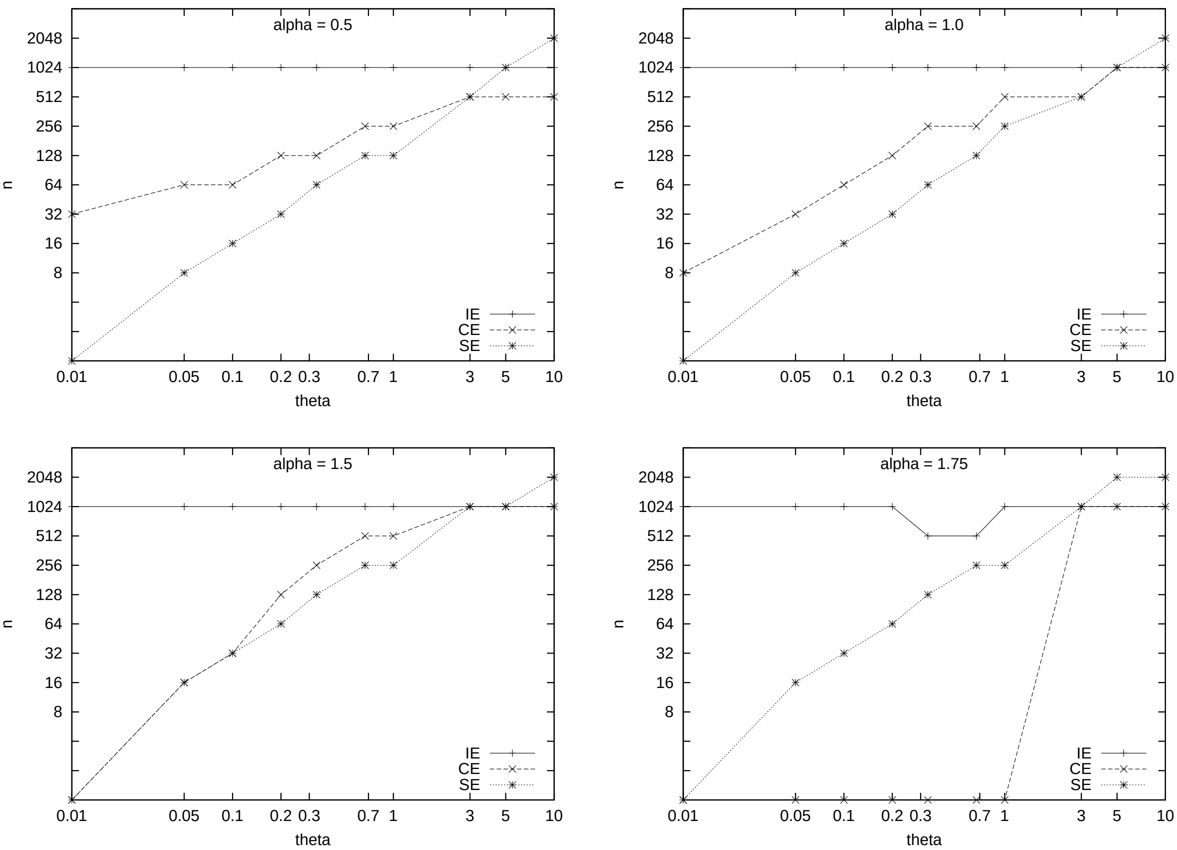

Figure 5: Current Computational Limits of Exact Simulation. We consider the simulation of intrinsically stationary Gaussian surfaces with powered exponential variogram, $\gamma(\mathbf{h}) = 1 - \exp(-|\theta \mathbf{h}|^{\alpha})$, on a square lattice in $[0,1]^2$ with spacing $1/n$ along each coordinate, using the standard circulant embedding (SE), cut-off embedding (CE) and intrinsic embedding (IE) techniques. For each method and for $\alpha = 0.50$, 1.00, 1.50 and 1.75, the associated graph divides the (n, θ) plane into a lower area, for which exact simulation is feasible, and an upper area, for which the method fails.

4.2 Current computational limits of exact simulation

The cut-off embedding and intrinsic embedding approaches push the computational limits of exact simulation. Figure 5 illustrates the current limits for random fields with powered exponential dependence structure. Specifically, we consider the simulation of an intrinsically stationary Gaussian random field with variogram $\gamma(\mathbf{h}) = 1 - \exp(-|\theta \mathbf{h}|^{\alpha})$ on a square lattice in $[0,1]^2$ with spacing $1/n$ along each coordinate. Assuming that we can apply the fast Fourier transform to square matrices of size at most $4\,096 \times 4\,096$, the graphs show the largest value of n for which exact simulation with the standard circulant embedding technique (SE), the cut-off embedding approach (CE) and the intrinsic embedding approach (IE) is feasible. For each technique and for $\alpha = 0.50, 1.00, 1.50$ and 1.75, respectively, the associated graph divides the (n, θ) plane into a lower area, for which exact simulation is feasible, and an upper area, for which the method fails. The intrinsic embedding approach applies very generally and allows for exact simulation on grids with spacing $1/512$ or larger for all parameter combinations that we considered. The cut-off embedding method outperforms

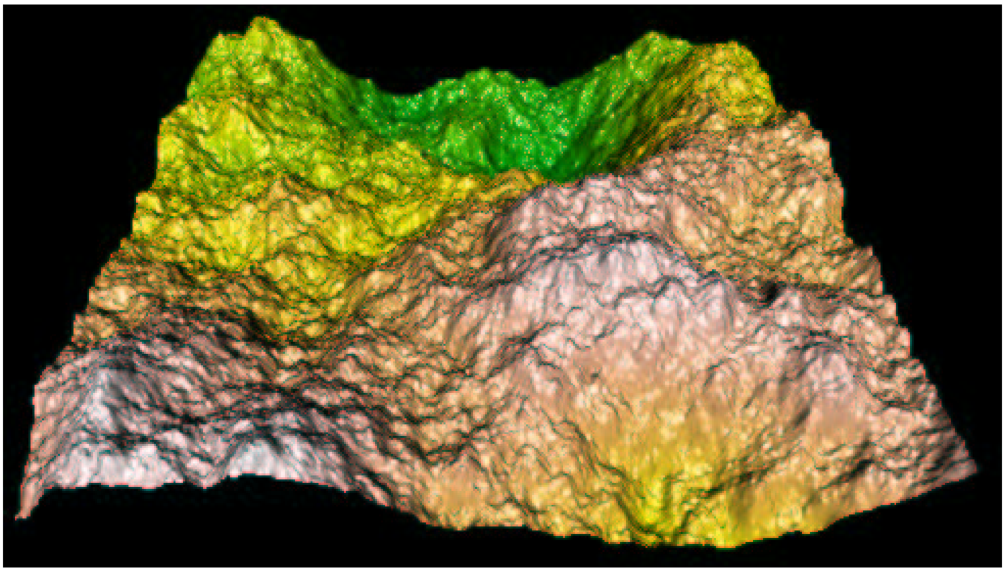

Figure 6: Exact Realization of a Gaussian Surface Using the Intrinsic Embedding Technique. The random field has powered exponential variogram, $\gamma(\mathbf{h}) = 1 - \exp(-|\mathbf{h}|^{1.75})$, and the simulation domain is a square grid in $[0,1]^2$ with spacing 1/512 along each coordinate.

the standard circulant embedding technique for various parameter combinations, particularly when α is small, but is not quite as applicable as the intrinsic embedding approach.

4.3 Example

Figure 6 shows a realization of an intrinsically stationary Gaussian surface with powered exponential variogram and parameter values $\alpha = 1.75$ and $\theta = 1$, respectively. The simulation domain is a square grid in $[0,1]^2$ with spacing 1/512 along each coordinate. The following commands were used to generate this surface with the RandomFields package using the intrinsic embedding technique:

```
InitGaussRF(x=c(0,1,1/512), y=c(0,1,1/512), grid=TRUE, gridtriple=TRUE,
            param=c(0,1,0,1,1.75), model="stable", method="intr")
surface <- DoSimulateRF(n=n)
```

Here, `n` is the desired number of simulations for the Gaussian surface. On our 512 MB RAM machine, the calls to the `InitGaussRF` and `DoSimulateRF` functions take 9 and $12 \cdot$ `n` seconds, respectively. The parameter `method="intr"` ensures the use of the intrinsic embedding technique, without invoking a prior search for a suitable simulation method. The visual display in Figure 6 uses functions implemented in the RGL visualization device system for the R language (Adler, Nenadić and Zucchini 2003). Neither the Cholesky decomposition nor the standard circulant embedding or the cut-off embedding approach provide exact simulations in this situation; see Figure 5.

References

Adler, D., Nenadić, O. and Zucchini, W. (2003). RGL: A R-library for 3D visualization with OpenGL. In *Proceedings of the 35th Symposium on the Interface: Computing Science and Statistics*. Available online at www.statoek.wiso.uni-goettingen.de/mitarbeiter/nenadic.html.

Besag, J. E. and Moran, P. A. P. (1975). On the estimation and testing of spatial interaction in Gaussian lattice processes. *Biometrika*, **62**, 555–562.

Caccia, D. C., Percival, D., Cannon, M. J., Raymond, G. and Bassingthwaighte, J. B. (1997). Analyzing exact fractal time series: evaluating dispersional analysis and rescaled range methods. *Physica A*, **246**, 609–632.

Chan, G. and Wood, A. T. A. (1997). An algorithm for simulating stationary Gaussian random fields. *Applied Statistics*, **46**, 171–178.

Chan, G. and Wood, A. T. A. (2000). Increment-based estimators of fractal dimension for two-dimensional surface data. *Statistica Sinica*, **10**, 343–376.

Chilès, J.-P. and Delfiner, P. (1999). *Geostatistics. Modeling Spatial Uncertainty*. Wiley, New York.

Craigmile, P. F. (2003). Simulating a class of stationary Gaussian processes using the Davies–Harte algorithm, with application to long memory processes. *Journal of Time Series Analysis*, **24**, 505–511.

Davies, S. and Hall, P. (1999). Fractal analysis of surface roughness by using spatial data (with discussion). *Journal of the Royal Statistical Society Ser. B*, **61**, 3–37.

Dietrich, C. R. (1993). Computationally efficient Cholesky factorization of a covariance matrix with block Toeplitz structure. *Journal of Statistical Computation and Simulation*, **45**, 203–218.

Dietrich, C. R. and Newsam, G. N. (1993). A fast and exact method for multidimensional Gaussian stochastic simulations. *Water Resources Research*, **29**, 2861–2869.

Dietrich, C. R. and Newsam, G. N. (1997). Fast and exact simulation of stationary Gaussian processes through circulant embedding of the covariance matrix. *SIAM Journal on Scientific Computing*, **18**, 1088–1107.

Diggle, P. J., Tawn, J. A. and Moyeed, R. A. (1998). Model-based geostatistics. *Applied Statistics*, **47**, 299–326.

Gel, Y., Raftery, A. E. and Gneiting, T. (2004). Calibrated probabilistic mesoscale weather field forecasting: The geostatistical output perturbation (GOP) method (with discussion and rejoinder). *Journal of the American Statistical Association*, **99**, 575–590.

Gneiting, T. (1998). Simple tests for the validity of correlation function models on the circle. *Statistics & Probability Letters*, **39**, 119–122.

Gneiting, T. (1999a). A Pólya type criterion for radial characteristic functions in $\mathbb{R}^2$. *Expositiones Mathematicae*, **17**, 181–183.

Gneiting, T. (1999b). Radial positive definite functions generated by Euclid's hat. *Journal of Multivariate Analysis*, **69**, 88–119.

Gneiting, T. (2001). Criteria of Pólya type for radial positive definite functions. *Proceedings of the American Mathematical Society*, **129**, 2309–2318.

Gneiting, T. (2002). Compactly supported correlation functions. *Journal of Multivariate Analysis*, **83**, 493–508.

Gneiting, T. and Schlather, M. (2004). Stochastic models that separate fractal dimension and the Hurst effect. *SIAM Review*, **46**, 269–282.

Golub, G. H. and van Loan, C. F. (1996). *Matrix Computations*, 3rd ed. John Hopkins University Press, Baltimore.

Gotway, C. A. (1994). The use of conditional simulation in nuclear-waste-site performance assessment (with discussion and rejoinder). *Technometrics*, **36**, 129–161.

Ihaka, R. and Gentleman, R. (1996). R: A language for data analysis and graphics. *Journal of Computational and Graphical Statistics*, **5**, 299–314.

Kozintsev, B. (1999). Computations with Gaussian random fields. Ph. D. Thesis, University of Maryland. Available online at techreports.isr.umd.edu/ARCHIVE/.

Matérn, B. (1986). *Spatial Variation*, 2nd edition. Springer, Berlin.

Rue, H. (2001). Fast sampling of Gaussian Markov random fields. *Journal of the Royal Statistical Society Ser. B*, **63**, 325–338.

Rue, H. and Held, L. (2005). *Gaussian Markov Random Fields: Theory and Applications.* Chapman and Hall/CRC Press, London.

Schlather, M. (2001). Simulation and analysis of random fields. *R News*, **1**, 18–20.

Ševčíková, H. (2004). Statistical simulations on parallel computers. *Journal of Computational and Graphical Statistics*, **13**, 886–906.

Stein, M. L. (1999). *Interpolation of Spatial Data. Some Theory for Kriging.* Springer, New York.

Stein, M. L. (2002a). Fast and exact simulation of fractional Brownian surfaces. *Journal of Computational and Graphical Statistics*, **11**, 587–599.

Stein, M. L. (2002b). Proofs for Stein (2002a). Available online at www.amstat.org/publications/jcgs under the 'Supplemental Materials Archive' link.

Whittle, P. (1954). On stationary processes in the plane. *Biometrika*, **41**, 434–449.

Wood, A. T. A. and Chan, G. (1994). Simulation of stationary Gaussian processes in $[0,1]^d$. *Journal of Computational and Graphical Statistics*, **3**, 409–432.

Zhu, Z. and Stein, M. L. (2002). Parameter estimation for fractional Brownian surfaces. *Statistica Sinica*, **10**, 343–376.